Available online at www.CivileJournal.org

Civil Engineering Journal

(E-ISSN: 2476-3055; ISSN: 2676-6957)

Vol. 7, No. 07, July, 2021

Seismic Fragility Curves for Performance of Semi-rigid Connections of Steel Frames

Mohamed Saadi [1*], Djarir Yahiaoui [1], Noureddine Lahbari [1], Bouzid Tayeb [1]

[1] *LGC-ROI, Civil Engineering Laboratory-Risks and Structures in Interactions, Department of Civil Engineering, Faculty of Technology,University of Batna 2, Batna 5000, Algeria.*

Received 29 March 2021; Revised 24 May 2021; Accepted 11 June 2021; Published 01 July 2021

Abstract

A steel frame with a semi-rigid connection is one of the most widely used structural systems in modern construction. These systems are cheap to make, require less time to construct and offer the highest quality and reliable construction quality without the need for highly skilled workers. However, these systems show greater natural periods compared to their perfectly rigid frame counterparts. This causes the building to attract low loads during earthquakes. In this research study, the seismic performance of steel frames with semi-rigid joints is evaluated. Three connections with capacities of 50, 70 and 100% of the beam's plastic moment are studied and examined. The seismic performance of these frames is determined by a non-linear static pushover analysis and an incremental dynamic analysis leading finally to the fragility curves which are developed. The results show that a decrease in the connection capacity increases the probability of reaching or exceeding a particular damage limit state in the frames is found.

Keywords: Semi-rigid Connection; Steel Frame; Pushover Analysis; Incremental Dynamic Analysis; Fragility Curve.

1. Introduction

The actual behavior of connections is conventionally ignored in steel frame. In reality, structural analysis of steel frames is usually performed assuming that the connections meet the perfect conditions of a pinned or rigid connection. Consequently, the calculations are somewhat simplified but the structural model does not show the actual structural response. Available experimental data [1-3] show that, on one hand, joints commonly considered to be hinges often exhibit quite high stiffness and rotational resistance. On the other hand, the joints which are generally considered to be stiff can develop bending deformation. These behavioural characteristics largely affect the frame response. In fact, in conventionally pin- joint frames, the real stiffness of the joint results to a more favourable distribution of bending moments in the beams, whereas the true deformability of the joint in nominally stiff frames influences negatively the frame vulnerability to second order effects [4].

In contrary, experimental research shows that the actual behaviour of connections is found in between of that perfectly pinned joint and completely rigid joint: these joints are named semi-rigid joints [5]. The simple models used in the current design procedure are clearly effective in analysing a large number of structures, but in many cases the correct assessment of the structural reliability requires the semi-rigid behaviour of joints to be accounted for. This is expected to improve the reliability of the structural response prediction, allowing it to benefit from the actual

* Corresponding author: m.saadi@univ-batna2.dz

http://dx.doi.org/10.28991/cej-2021-03091714

behaviour of the joints. In fact, many studies [6-8] pointed out the economic benefits that can result from a design considering the real behaviour of beam-to-column joints. De Alvarenga (2020) [9] suggested new numerical formulation that integrates the behaviour of the plastic zone finite element model for semi-rigid steel frames. However, Astaneh and Nader (1992) and Mazzolani and Piluso (2012) [10, 11] have provided some attempts to codify the semi rigidity for seismic steel structures, and the evidence of the positive effect of semi-rigid joints in such structures is continuously increasing.

According to the new generation of European seismic codes, e.g., the ECCS Manual and Eurocode 8 [12, 13], a clear distinction is made between dissipative and non-dissipative structures. Non dissipative structures must resist to the most severe seismic movement within the elastic range, while dissipative structures are designed by allowing deformation to occur in predefined zones. During an earthquake, these zones must dissipate energy through hysteretic ductile behaviour in the plastic range. The formation of an appropriate dissipative mechanism is related to the topology of the structure and proper dimensioning.

Unbraced frames are used quite widely in areas affected by strong earthquakes for low and medium height buildings due to their high ductility. They generally provide a good energy dissipation capacity as a result of the hysterical ductile behaviour of the beams elements composing these frames. It is also possible for inelastic cyclic deformations to occur in other elements, such as connections .However, although the reputation of steel frames is well established, the vulnerability of unbraced frames became apparent during the powerful El Centro1940, Northridge 1994 and Kobe 1995 earthquakes, through brittle failures detected at the connections beams to columns of the structures [14]. Other studies include, the monotonic, cyclic, and dynamic behaviors of several types of semi-rigid joints were explored in Nader et al. (1996) [15]; and it was claimed that these joints are able to dissipate energy due to their relatively enlarged moment rotation hysteresis loops, which work as damping mechanism in steel frame.

One of the first experimental studies on the seismic behaviour of semi-rigid steel frame was published by Elnashai et al. (1998) [16]. It was shown that, when correctly designed, semi-rigid joints can perform similarly or even better than their fully rigid counterparts under a variety of loading conditions. Aksoylar et al. (2011) [17] studied the behaviour of structures with energy dissipation zones in semi-rigid joints designed in high seismicity locations and their seismic response was estimated analytically with various connection capacities. By using semi-rigid energy dissipating joints, it eliminates the necessity of the weak beam from the strong column and allows the use of more economical column sections. Razavi and Abolmaali (2014) [18] examined semi-rigid and rigid connections in high-rise steel construction, and observed that semi-rigid frames were more efficient than fully rigid frames. Faridmehr et al. (2017) [19] studied the seismic response of steel frames with semi-rigid joints and found that the more flexible the semi-rigid joint, the more the base shear demand decreases during the earthquake. Moussemi et al. (2017) [20], based on free vibration analysis, found the dynamic parameters of a two-story frame, in which the beam-column joints were modeled using semi-rigid connections.

Recently, Koriga et al. (2019) [21] studied the dynamic response of rigid and semi-rigid joints of steel frame under dynamic loads. The novelty introduced in the nonlinear model is to consider a unique bar element that represents the semi-rigid connection. Thus, there is no need to discretize the structural element (member) in the computer program where nonlinearity is taken into account by a flexibility factor in the stiffness matrix. Mahmoud and Elnashai (2013) [22] worked on a new hybrid system-level simulation application for seismic evaluation of steel frames with TSADWA connections. Sharma et al. (2021) [23] studied in detail the effects of semi-rigid joints using a variety of response parameters for a set of far-field and near-field earthquakes with directivity and flutter step employing nonlinear time history analysis. Hassan et al. (2020) [24] worked on the seismic response of semi-rigid steel frames exposed to actual main and aftershock ground motion with different connection capacities. Kiani et al. (2016) [25] developed fragility curves for three- and five-story building models composed of unbraced frames with masonry infill walls. Finally, Guettafi et al. (2021) [26] developed an equation to assist engineers in the design and response of soil-pile-structure interaction. The results of this formula allowed harmonization with the results of the fragility curves.

In this research study, the seismic response of steel frames with semi-rigid joints is estimated. Three semi-rigid moment-resisting frames with bolted connection with capacities of 50, 70 and 100% of the beam plastic moment are studied and examined. The seismic performance of these frames is determined by a non-linear static pushover analysis and an incremental dynamic analysis leading finally to the establishment of fragility curves.

2. Model Description

This study examines three frames with bolted joints at the ends representing 50, 70 and 100% of the beam's plastic moment capacity. The frames consist of five, seven, and ten stories with three spans of 4 m width and 3 m height, respectively. A similar elevation of frame is shown in Figure 1. It should be noted that the loads used is a dead load of 30 KN/m including the dead weight of the frame. The same gravity loads are considered for all floors. The structural steel used in this research is type S235 for the beams and columns.

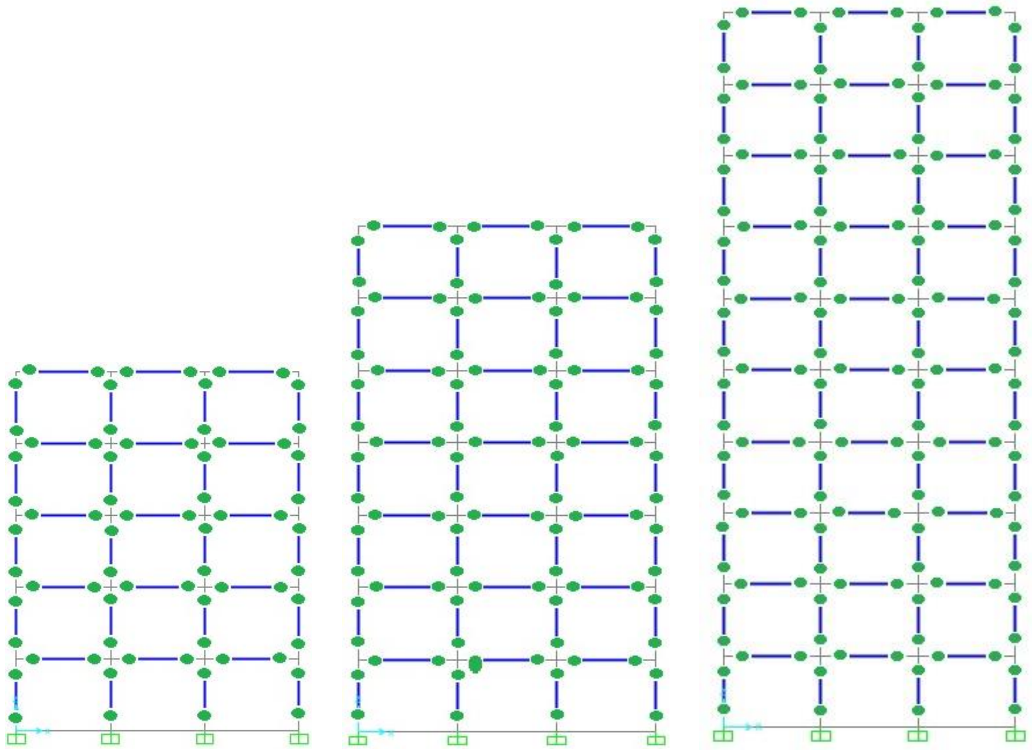

(a) (b) (c)

Figure 1. View of the sample steel frames (a) 5 stories (b) 7 stories (c) 10 stories

To model the joint, the standard nonlinear software SAP2000 [27] is employed. In this software, a multi-linear plastic connection element with zero length joints is applied. The joint shows kinematic hysteresis behaviour. The moment-rotation behavior curve of the joint is shown in Figure 2(a).

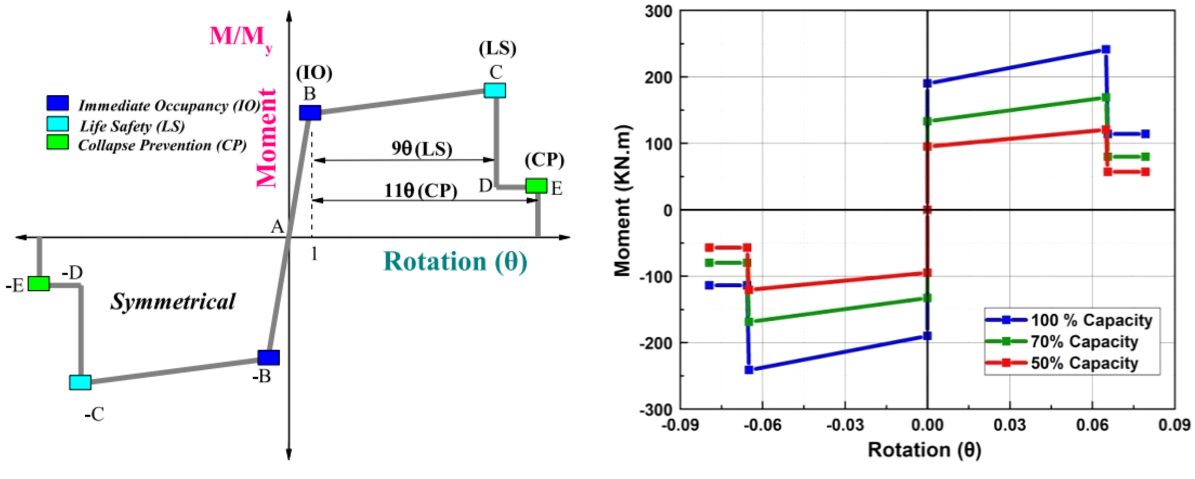

(a) (b)

Figure 2. Hysteresis curves for (a) Flexural default plastic hinges [23] (b) flexural plastic hinges used [27]

Material nonlinearity in steel frames is modeled as plastic hinges concentrated at the end of flexural hinges. Here, the standard plastic hinges contained by default in SAP2000, in accordance with the guidelines of Eurocode 3 [28], are used to capture the material nonlinearity. Type M3 and type P-M3 hinges are used for beams and columns, respectively, and are inserted at an equal absolute value of 0.05 of the member end length. Three limits states, namely "IO" immediate occupancy, "LS" life safety and "CP" collapse prevention for the default hinges are being considered [29], Figure 2(b) shows hysteresis curve for flexural plastic hinges used in this work study. Table 1 shows the details for the sections used in the frame and acceptance criteria.

Table 1. Dimensions of beam and column and acceptance criteria of rotation and translation displacement

Story	Components	Connection Capacity (%)	Sections	Hinge	Moment plastic	Acceptance Criteria		
						IO	LS	CP
5 Story	Column	100	HE 240A	P + M3	225.36	0.001	0.005	0.005
		70	HE 220A	P + M3	171.82	0.001	0.005	0.005
		50	HE 180A	P + M3	98.31	0.001	0.005	0.005
	Beam	100	IPE 270	M3	146.41	0.008	0.072	0.088
		70		M3	102.49	0.007	0.063	0.077
		50		M3	73.2	0.007	0.063	0.077
7 Story	Column	100	HE 260A	P + M3	278.30	0.001	0.005	0.005
		70	HE 240A	P + M3	225.36	0.001	0.005	0.005
		50	HE 200A	P + M3	129.77	0.001	0.005	0.005
	Beam	100	IPE 300	M3	189.97	0.007	0.063	0.077
		70		M3	132.98	0.007	0.063	0.077
		50		M3	94.98	0.007	0.063	0.077
10 Story	Column	100	HE 320A	P + M3	492.47	0.001	0.005	0.005
		70	HE 240A	P + M3	225.36	0.001	0.005	0.005
		50	HE 200A	P + M3	129.77	0.001	0.005	0.005
	Beam	100	IPE 300	M3	189.97	0.007	0.063	0.077
		70		M3	132.98	0.007	0.063	0.077
		50		M3	94.98	0.007	0.063	0.077

3. Research Methodology

The flowchart of the research and characterization methodology is depicted in Figure 3

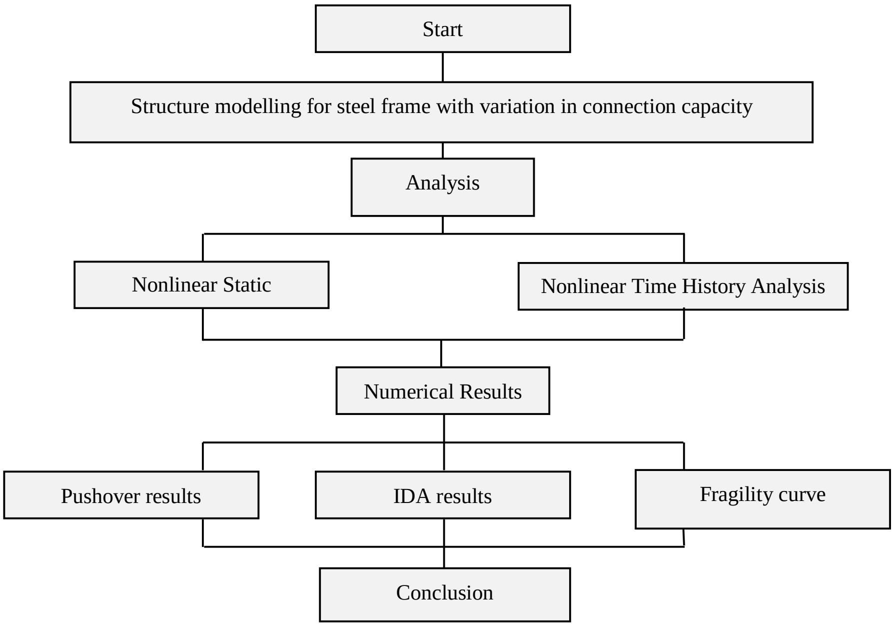

Figure 3. Flowchart of the research study

3.1. Nonlinear Static Pushover Analysis

Pushover analysis is an approach method in which the frame is exposed to monotonic increasing lateral force with an unchanging height-width partition until a target displacement is achieved. Hence, the method consists of a variety of sequential elastic analyses, overlaid to approach the force-displacement curve of the global structure. A two- or three-dimensional model comprising of bilinear or trilinear load-deformation diagrams of all lateral force withstanding elements is first generated and the gravity loads are initially applied [30]. The pushover analysis method is shown in Figure 4.

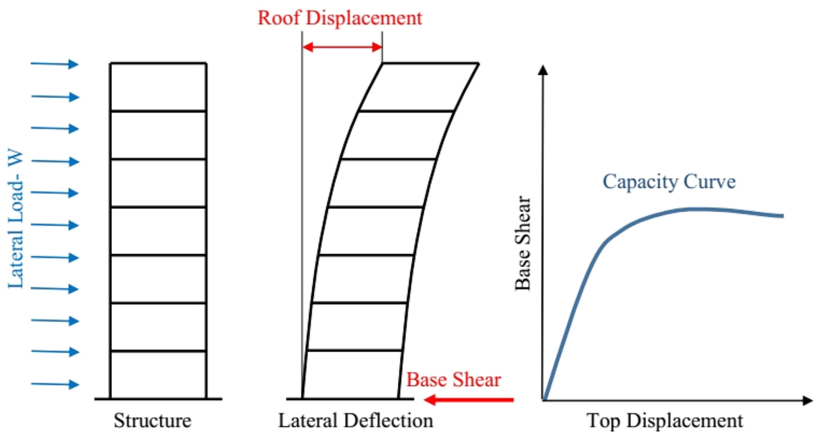

Figure 4. Pushover analysis method [31]

3.2. Ground Motions used in the Dynamic Analysis

The selection of an appropriate parameter that reflects the intensity of ground motion is a difficult operation in the analysis of the probability of the seismic potential. This parameter should not only express the gravity of an earthquake, but should also be related to the damage to structures and elements. The ideal measures must satisfy several recognized criteria: satisfaction, practicability, calculability and effectiveness [32]. In one term, a selected intensity value must make engineering sense and be independent of ground motion characteristics with a total variety of structural response for IM in a reasonable range for different types of structures.

An appropriate set of ground motions is necessary to execute the incremental dynamic analysis. As suggested by Eurocode 8 and by Bommer and Scott (2000) [33], a minimum of seven ground motions should be used to represent the behavior of a building. However, for mid-rise buildings, ten to twelve ground motions are needed to obtain a reliable evaluation of the seismic demand [34]. FEMA P695 [35] recommends a minimum of twenty ground motions to realize incremental dynamic analysis and elaborate fragility curves. The ground motions can be necessary selected from real earthquake records or artificially generated. In fact, real earthquakes are more realistic because they include all the ground motion information's, such as duration, energy content, frequency, amplitude, phase and number of cycles [36]. Accordingly, twenty earthquake records from many regions were employed to perform the incremental dynamic analysis. Details of the 20 record of ground motion which were selected are presented in Table 2.

Table 2. Ground Motions used in the dynamic analysis

No.	Year	Earthquake	M	Country	PGA
1	1976	Friuli	6.5	Italy	0.25
2	1961	Hollister	5.6	USA	0.17
3	1979	Imperial Valley	6.5	USA	0.38
4	1995	Kobe	6.9	Japan	0.212
5	1999	Kocaeli	7.5	Turkey	0.358
6	1992	Landers	7.3	USA	0.42
7	1983	Trinidad	5.8	Trinidad and Tobago	0.33
8	1994	Newhall	6.7	USA	0.605
9	1994	Santa Monica	6.7	USA	0.228
10	1979	Elcentro	6.5	USA	0.40
11	1979	Array-06	6.5	USA	0.43
12	1989	Corralitos	6.9	USA	0.483
13	1987	Lacc North	5.9	USA	0.25
14	1989	Lexington	6.9	USA	0.4
15	1994	Sylmar	6.7	USA	0.578
16	1992	Lucerne	7.3	USA	0.60
17	1992	Petrolia	7.2	USA	0.18
18	1992	Yermo	7.3	USA	0.154
19	1989	Oakland_Outher	6.9	USA	0.42
20	1988	Pomona	7.5	USA	0.34

Figure 5 shows the result the simulation of twenty acceleration records in the form of response spectrum curves and the target response spectrum. To match these ground motions, the Seismo-Match software [37] is used. This software program can adjust the ground motion records to match a particular target response spectrum [37].

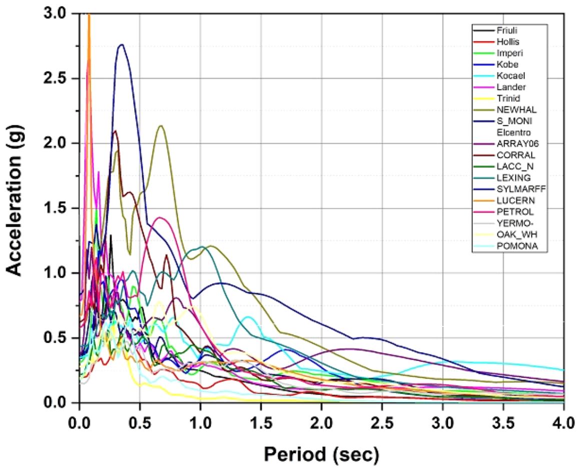

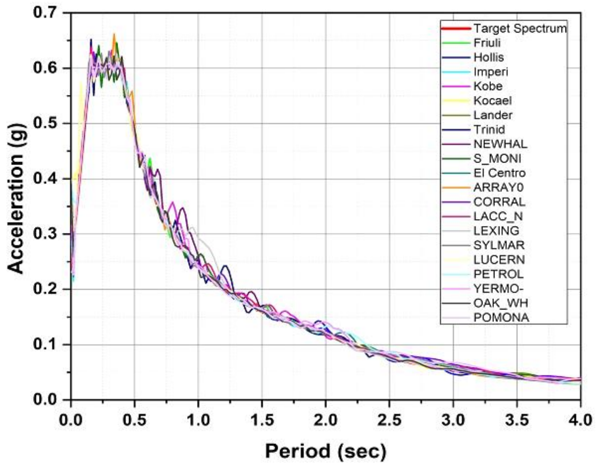

Figure 5. Matched spectrums by Seismo-match

Table 3 shows the value of fundamental period and the different acceleration projection on spectrum acceleration with variation in connection capacity (50, 70, and 100%)

Table 3. The values of the fundamental periods and their corresponding acceleration

	5 Story			7 Story			10 Story		
	100%	**70%**	**50%**	**100%**	**70%**	**50%**	**100%**	**70%**	**50%**
Period T_f	1.43	1.55	1.90	1.73	1.84	2.21	2.23	2.64	3.17
Ag (T_f) (g)	0.17	0.15	0.13	0.14	0.13	0.10	0.10	0.07	0.05

3.3. Incremental Dynamic Analysis IDA

IDA is a method of computer analysis employed to evaluate structures subjected to increasing seismic loads. In this approach, the seismic risk for this structure is estimated by a probabilistic seismic analysis [38]. The IDA allows for multiple nonlinear time history analysis of the structure being studied by applying a set of specified ground motions. Each earthquake is scaled to generate a specific seismic intensity. Nonlinear dynamic analysis is achieved by applying each ground motion record many at various scales. The scaling is performed that the structure is subjected to a wide range of behaviours, from elastic to inelastic, and eventually to a global dynamic instability represented by a total collapse. Figure 6 shows the IDA method.

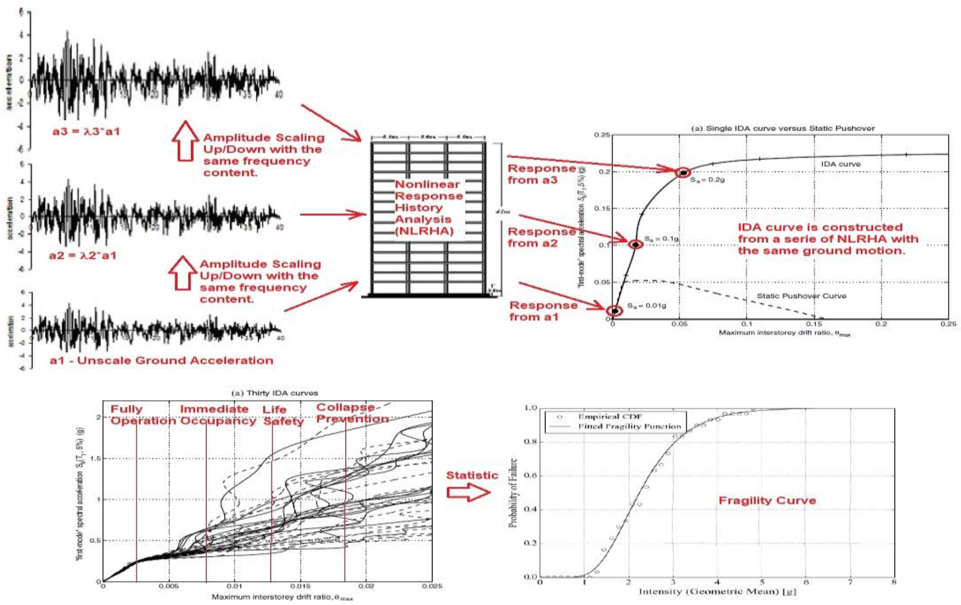

Figure 6. Incremental dynamic analysis method [35]

The analysis discussed in this section focuses on the three limits states, namely the immediate occupancy, life safety, and collapse prevention. In order to quantify the level of damage corresponding to each of these three states, the inter story drift ratio was considered as a non-cumulative damage index as mentioned by FEMA356 [39]. The values of the maximum inter-story drift ratios used to evaluate damage are 0.5, 1.5, and 2% for the immediate occupancy, life safety, and collapse prevention states, respectively.

Nonlinear time history analysis by means of SAP 2000 software was performed on each structure using some ground motion with maximal ground acceleration, PGA scaled incrementally to 1.0g using a 0.1g step. The maximum inter-stage drift ratio was determined for each PGA, which represents a point on the IDA curve. The points of this drift ratio result from the various PGA values form the complete IDA curve for a specific ground motion. The procedure was iterated for the 20 ground motions employed in this study. All curves of IDA for these 20 ground motions characterize the seismic performance of a specific structural model.

3.4. Fragility Function

Fragility curves represent the probability of structural damage from earthquakes as a function of different ground motion indices. In the present paper, the fragility curves are established in terms of acceleration. It is supposed that the fragility curves can be represented as a two-parameter lognormal distribution functions [40]. Based on this theory, the cumulative probability of damage occurrence, equal to or higher than damage level D, is given by the following equation.

$$P(IM = x) = \Phi\left[\frac{\ln(x/\mu)}{\sigma}\right] \tag{1}$$

where *P(IM=x)* is the probability that a ground motion with $IM = x$ will cause the structure to collapse, Φ is the standard normal cumulative distribution function (CDF), μ is the median of the fragility and σ is the standard deviation.

4. Results and Discussions

The assessment of the frames is conducted using static pushover analysis, and non-linear IDA and fragility curve. In this section, all the results are summarized, interpreted, and discussed.

4.1. Pushover Results

Figure 7 shows the lateral response of steel frame with connection capacity equal to 50, 70, and 100% of the plastic moment capacity of the respective beams for 5 story, 7 story and 10 story frames.

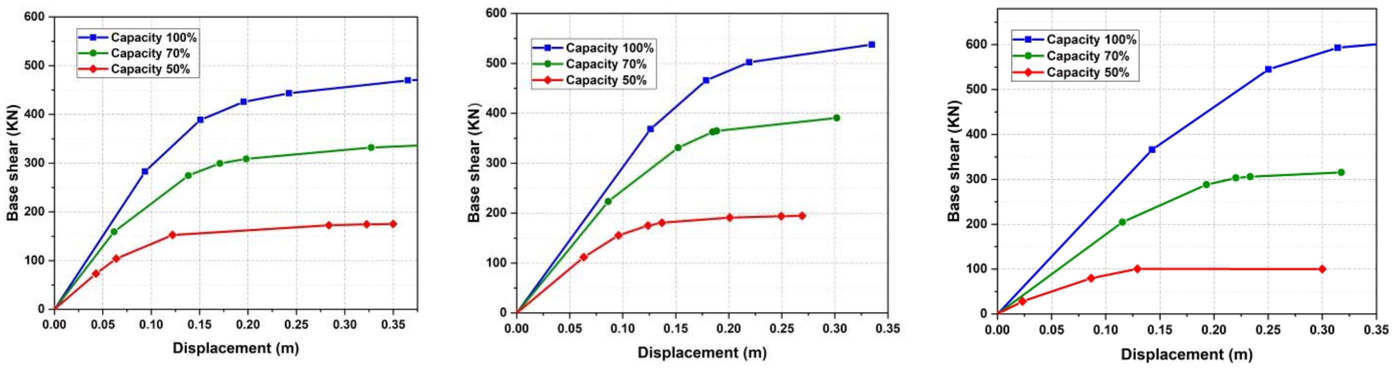

a-5 Story **b-7 Story** **c-10 Story**

Figure 7. Lateral load–displacement response with variation in connection capacity (50, 70 and 100%) and steel frame story

The results show that the lateral capacity of model with connection capacity equal to 50%, 70%, decreases in comparison with rigid model (100%) with values of (63.7%, 28%) for 5 stories, (63%, 27%) for 7 stories and (84%, 51%) for 10 stories. The results leading to that of the model with connection capacity 50, 70%, indicate that the ductility increases 16.4% and 29% for 5 stories, 32% and 9.7% for 7 stories and 98% and 11.6% for 10 stories compared to the rigid model.

4.2. Incremental Dynamic Analysis

Figure 8 shows the IDA results for steel frame with variation connection capacity of 50, 70, and 100% of the plastic moment capacity for the respective beams for five- story, seven- story and ten- story frames, respectively.

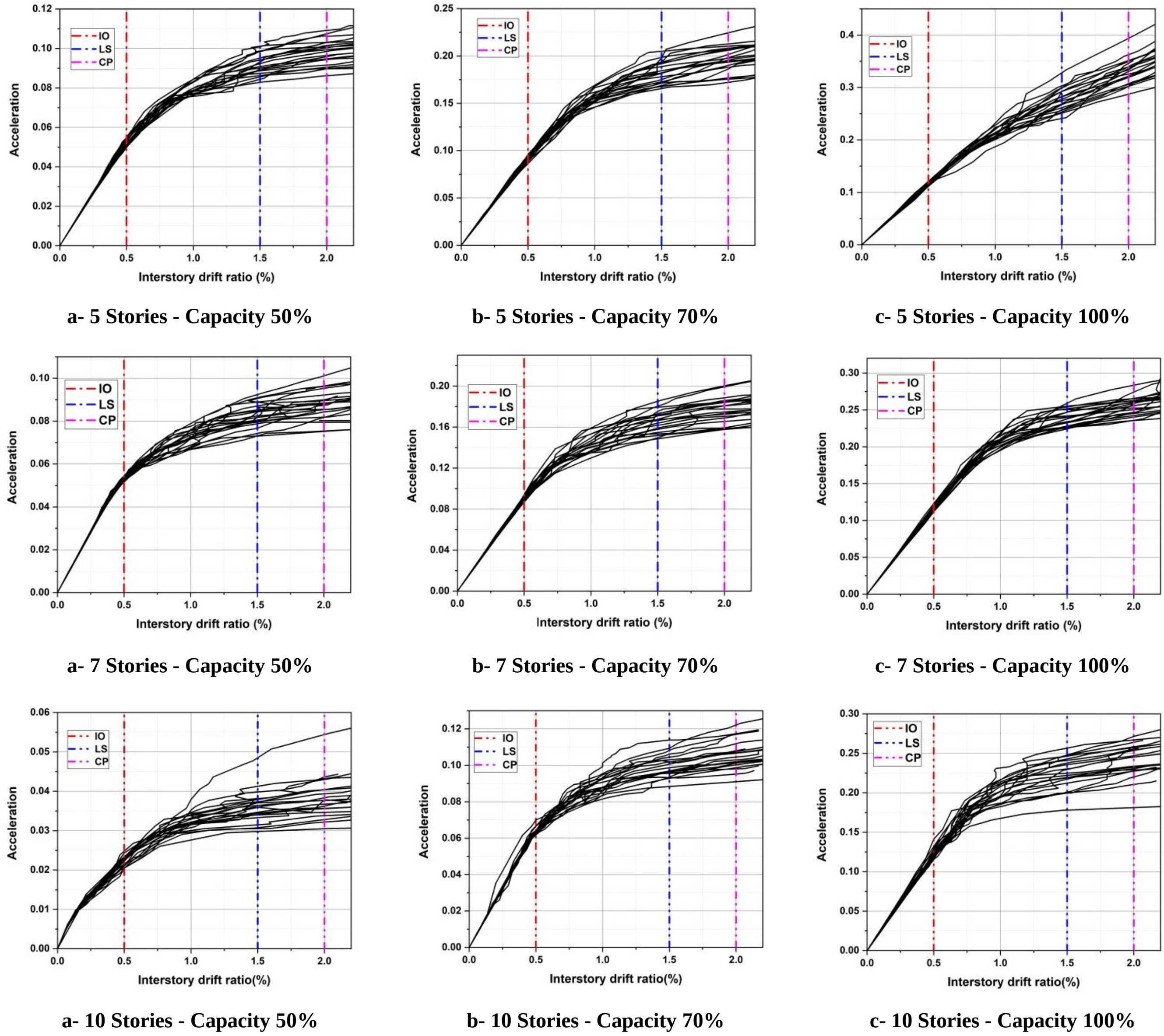

a- 5 Stories - Capacity 50% **b- 5 Stories - Capacity 70%** **c- 5 Stories - Capacity 100%**

a- 7 Stories - Capacity 50% **b- 7 Stories - Capacity 70%** **c- 7 Stories - Capacity 100%**

a- 10 Stories - Capacity 50% **b- 10 Stories - Capacity 70%** **c- 10 Stories - Capacity 100%**

Figure 8. Generated IDA for models with variation in connection capacity (50, 70, and 100%) and steel frame story

It is observed that the behaviour of all steel frames is linear when the inter-story drift ratio is less than 0.5%. And when the capacity of the connection decreases, the spectral acceleration is decreased by 20 and 70 % for connection capacity equal to 50, 70% respectively. When the inter-story drift ration increases the spectral acceleration is increased compared to connection capacity equal to 50%.

The increase in number of stories leads to a decrease of the spectral acceleration when compared to 5 stories, 10 to 20%, for 7 stories, and 60 to 40% for 10 stories for connection capacity of 50, 70 and 100% respectively. This is due to the augmentation of period of structures.

4.3. Fragility Curves

Figures 9 shows the fragility curves for steel frame with five stories and variation in connection capacity (50, 70, and 100%).

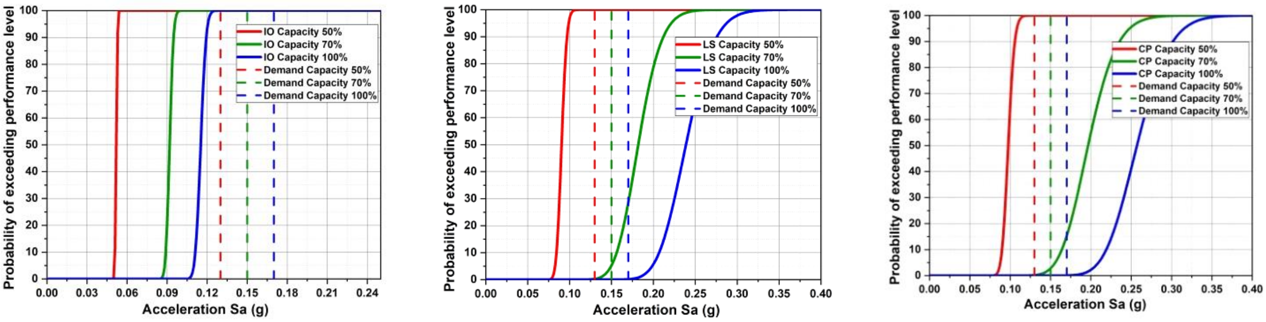

Immediate occupancy **Life Safety** **Collapse Prevention**

Figure 9. Fragility curves for steel frame of five stories and variation in connection capacity (50, 70, and 100%)

The decrease of the value of connection capacity indicates that the probability of exceedance for each damage state is increased and is affected by different damage states. The five story steel frame with capacity connection of 50% is more vulnerable than 70 and 100%. The values of Sa (50%) of probability of damage of steel frame with connection capacity, gives a reduction compared to a connection capacity 100%. In order of 54, 62, 60% for connection capacity equal to 50% and 21, 25, and 20% for connection capacity equal to 70%; for all limit states due to the decrease in moment plastic.

Figure 10 shows the Probability of Exceedance (POE) for five-story frame for different accelerations Ag(Tf) giving through projection the value of fundamental period on spectrum acceleration with variation in connection capacity (50, 70, and 100%) for different damage states (IO, LS, CP).

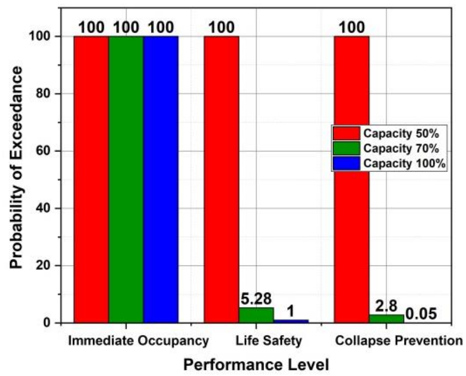

Figure. 10. Probability of Exceedance (POE) for five-stories with Ag(T_f)

The highest POE is provided by connection capacity of 50% in the order of 100% at 0.13g for all limit states. For connection capacity of 70% in the order of 100%, 5.28% and 2.8% at 0.15g for IO, LS CP respectively. Finally for connection capacity of 100% in the order of 100%, 1% and 0.05% at 0.17g for IO, LS CP respectively.

Figure 11 shows the fragility curves for steel frame with seven stories and variation in connection capacity (50, 70, and 100%). The results for a seven-story steel frame give the same results as for a five-story steel frame, but with an increase in the value of acceleration for the probability of damage 50% in life safety and collapse prevention limit states.

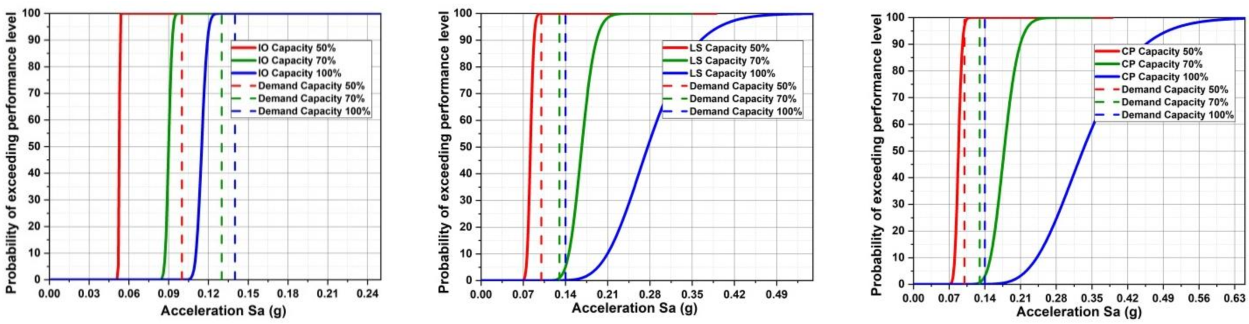

Immediate occupancy **Life Safety** **Collapse Prevention**

Figure 11. Fragility curves for steel frame of seven stories and variation in connection capacity (50, 70, and 100%)

Figure 12 shows the Probability of Exceedance (POE) for seven-stories for different accelerations Ag(T_f) giving through projection the value of fundamental period on spectrum acceleration with variation in connection capacity (50, 70, and 100%) for different damage states (IO, LS, CP).

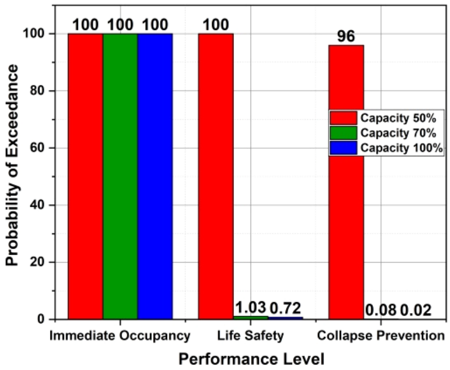

Figure 12. Probability of Exceedance (POE) for seven-stories with Ag(T_f)

The highest POE is provided by connection capacity of 50% in the order of 100% at 0.10g for all limit states, for connection capacity of 70% in the order of 100%, 5.28% and 2.8% at 0.13g for IO, LS CP respectively. And for connection capacity of 100% in the order of 100%, 1% and 0.05% at 0.14g for IO, LS CP respectively.

Figures 13 shows the fragility curves for ten story steel frame and variation in connection capacity (50%, 70%, and 100%). The results for a ten-story steel frame give the same results as for a five-story and seven-story steel frames, but with a decrease in the value of acceleration for the probability of damage 50% in life safety and collapse prevention limit states.

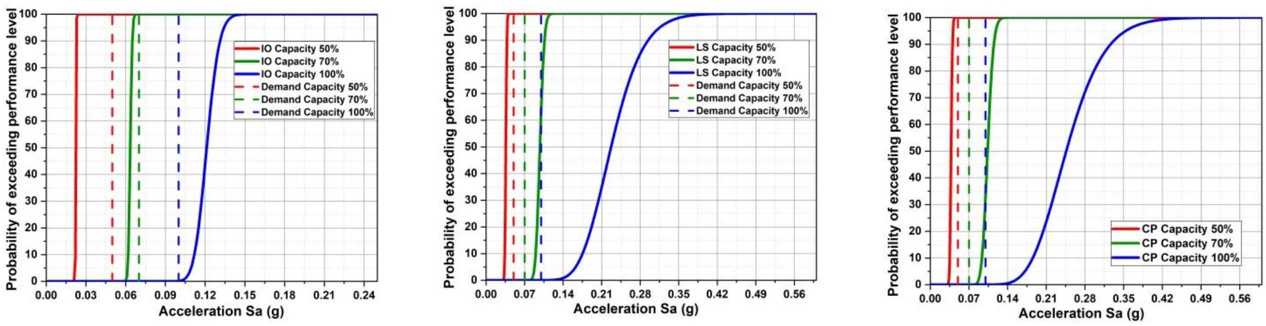

Immediate occupancy **Life Safety** **Collapse Prevention**

Figure 13. Fragility curves for steel frame of ten story and variation in connection capacity (50, 70, and 100%)

Figure 14 shows the Probability of Exceedance (POE) for ten-story frame for different accelerations Ag(T_f) giving through projection the value of fundamental period on spectrum acceleration with variation in connection capacity (50, 70, and 100%) for different damage states (IO, LS, CP).

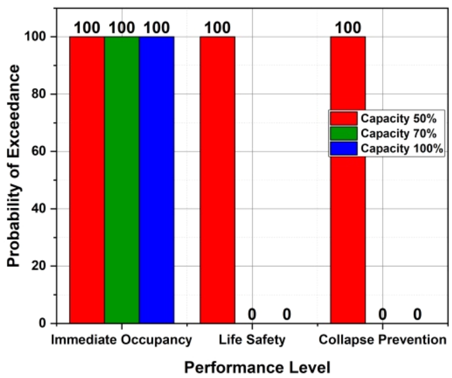

Figure 14. Probability of Exceedance (POE) for ten-story frame with Ag(T_f)

The highest POE is provided by connection capacity of 50% in the order of 100% at 0.05g for all limit states, for connection capacity of 70% in the order of 100% for IO and zero percent for LS and CP at 0.07g. For connection capacity of 100% of the order of 100% for IO and zero percent for LS and CP at 0.10g.

5. Conclusions

In this study, three frames with bolted joints representing 50%, 70% and 100% of the beam's plastic moment capacity, were investigated under earthquake loading. Pushover and the incremental dynamic analyses were carried for the three steel frames (five, seven and ten stories) for developed the fragility curves were compared, and the important findings inferred from the study are enumerated as follows:

- The results show that the lateral capacity decreases and the ductility increases when the connection capacity is decreased, because semi-rigid connections of steel frames show greater natural periods compared to their perfectly rigid frame counterparts. This causes the building to attract low loads during earthquakes;
- The steel frame with connection capacity of 50% is highly vulnerable for all types of frames;
- The steel frame with connection capacity of 70% slows vulnerability and damage for all types of frames, which gives a good result;
- The diminution in capacity of the connection leads to a decrease of the spectral acceleration;
- The increase in the number of stories leads a decrease in spectral acceleration.

Therefore, the design of steel frame with semi-rigid connection should provide adequacy with the consideration to the two demand measures, MIDR and MID, especially under NFD-HR and NFFS earthquakes.

6. Declarations

6.1. Author Contributions

The basic theme of the research was discussed and decided by all authors. The manuscript was written by S.M. and Y.D. while the numerical analysis work was carried out by L.N. and T.B., the results, discussions and conclusion section was completed by all authors. All authors have read and agreed to the published version of the manuscript.

6.2. Data Availability Statement

The data presented in this study are available in article.

6.3. Funding

The authors received no financial support for the research, authorship, and/or publication of this article.

6.4. Conflicts of Interest

The authors declare no conflict of interest.

7. References

[1] Goverdhan, Arvind Vasant. "A collection of experimental moment-rotation curves and evaluation of prediction equations for semi-rigid connections." PhD diss., Vanderbilt University, (1983).

[2] Nethercot, D. A. Steel beam to column connections-a review of tests data. CIRIA, Construction Industry Research and Information Assoc., (1985).

[3] Chen, Wai‐Fah, and N. Kishi. “Semirigid Steel Beam‐to‐Column Connections: Data Base and Modeling.” Journal of Structural Engineering 115, no. 1 (January 1989): 105–119. doi:10.1061/(asce)0733-9445(1989)115:1(105).

[4] Chen, Wai-Fah, Yoshiaki Goto, and JY Richard Liew. Stability design of semi-rigid frames. John Wiley & Sons, (1995).

[5] Yang, Cheol Min, and Young Moon Kim. “Cyclic Behavior of Bolted and Welded Beam-to-Column Joints.” International Journal of Mechanical Sciences 49, no. 5 (May 2007): 635–649. doi:10.1016/j.ijmecsci.2006.09.022.

[6] Bjorhovde, Reidar. "Effect of end restraint on column strength-practical applications." Engineering Journal-American Institute of Steel Construction Inc 21, no. 1 (1984): 1-13.

[7] Anderson, D., A. Colson, and Jean-Pierre Jaspart. "Connection and frame design for economy." Bouwen met Staal: Kwartaaltijdschrift Gewijd aan Staal en Staalconstructies (1994): 34-38.

[8] Faella, C., V. Piluso, and G. Rizzano. “A New Method to Design Extended End Plate Connections and Semirigid Braced Frames.” Journal of Constructional Steel Research 41, no. 1 (January 1997): 61–91. doi:10.1016/s0143-974x(97)00001-1.

[9] De Alvarenga, Arthur Ribeiro. "Plastic-Zone Advanced Analysis – Formulation Including Semi-Rigid Connection." Engineering Structures 212 (June 2020): 110435. doi:10.1016/j.engstruct.2020.110435.

[10] Astaneh, A., and N. Nader. "Proposed Code Provision for Sesimic Design of Steel Semirigid Frames." submitted to AISC Engineering Journal for review and publication (1992).

[11] Mazzolani, Federico, and Vincenzo Piluso. "Theory and Design of Seismic Resistant Steel Frames" (September 10, 2012). doi:10.1201/9781482271348.

[12] Mazzolani, F. M., and V. Piluso. "ECCS manual on design of steel structures in seismic zones." ECCS Publication (1994): 1-60.

[13] European Committee for Standardization. Eurocode 8: Design Provisions for Earthquake Resistance of Structures. Central Secretariat, CEN, 1994. doi:10.3403/00749165u.

[14] Mazzolani, Federico, ed. "Moment Resistant Connections of Steel Frames in Seismic Areas" (April 27, 2000). doi:10.1201/9781482289077.

[15] Nader, Marwan N., and Abolhassan Astaneh-Asl. "Shaking Table Tests of Rigid, Semirigid, and Flexible Steel Frames." Journal of Structural Engineering 122, no. 6 (June 1996): 589–596. doi:10.1061/(asce)0733-9445(1996)122:6(589).

[16] Elnashai, A. S., A. Y. Elghazouli, and F. A. Denesh-Ashtiani. "Response of Semirigid Steel Frames to Cyclic and Earthquake Loads." Journal of Structural Engineering 124, no. 8 (August 1998): 857–867. doi:10.1061/(asce)0733-9445(1998)124:8(857).

[17] Aksoylar, Nihan Doğramacı, Amr S. Elnashai, and Hussam Mahmoud. "The Design and Seismic Performance of Low-Rise Long-Span Frames with Semi-Rigid Connections." Journal of Constructional Steel Research 67, no. 1 (January 2011): 114–126. doi:10.1016/j.jcsr.2010.07.001.

[18] Razavi, Mohammad, and Ali Abolmaali. "Earthquake Resistance Frames with Combination of Rigid and Semi-Rigid Connections." Journal of Constructional Steel Research 98 (July 2014): 1–11. doi:10.1016/j.jcsr.2014.02.006.

[19] Faridmehr, Iman, Mahmood Md. Tahir, Tom Lahmer, and Mohd Hanim Osman. "Seismic Performance of Steel Frames with Semirigid Connections." Journal of Engineering 2017 (2017): 1–10. doi:10.1155/2017/5284247.

[20] Moussemi, Mojtaba, Davoud Nezamolmolki, and Ahmad Aftabi Sani. "Dynamic Investigation of a Two Story-Two Span Frame Including Semi-Rigid Khorjini Connections." International Journal of Steel Structures 17, no. 4 (December 2017): 1471–1486. doi:10.1007/s13296-017-1216-7.

[21] Koriga, S., A.N.T. Ihaddoudene, and M. Saidani. "Numerical Model for the Non-Linear Dynamic Analysis of Multi-Storey Structures with Semi-Rigid Joints with Specific Reference to the Algerian Code." Structures 19 (June 2019): 184–192. doi:10.1016/j.istruc.2019.01.008.

[22] Mahmoud, Hussam, and Amr Elnashai. "Hybrid Simulation of Semi-Rigid Partial-Strength Steel Frames." Structures Congress 2013 (April 30, 2013). doi:10.1061/9780784412848.210.

[23] Sharma, Vijay, Mahendra Kumar Shrimali, Shiv Dayal Bharti, and Tushar Kanti Datta. "Seismic Fragility Evaluation of Semi-Rigid Frames Subjected to Near-Field Earthquakes." Journal of Constructional Steel Research 176 (January 2021): 106384. doi:10.1016/j.jcsr.2020.106384.

[24] Hassan, Emad M., Sushant Admuthe, and Hussam Mahmoud. "Response of Semi-Rigid Steel Frames to Sequential Earthquakes." Journal of Constructional Steel Research 173 (October 2020): 106272. doi:10.1016/j.jcsr.2020.106272.

[25] Kiani, Amir, Babak Mansouri, and Abdolreza S. Moghadam. "Fragility Curves for Typical Steel Frames with Semi-Rigid Saddle Connections." Journal of Constructional Steel Research 118 (March 2016): 231–242. doi:10.1016/j.jcsr.2015.11.001.

[26] Guettafi, Nesrine, Djarir Yahiaoui, Khelifa Abbeche, and Tayeb Bouzid. "Numerical Evaluation of Soil-Pile-Structure Interaction Effects in Nonlinear Analysis of Seismic Fragility Curves." Transportation Infrastructure Geotechnology (April 8, 2021). doi:10.1007/s40515-021-00161-y.

[27] SAP2000, Version 21. "Basic analysis reference". Computers and Structures, Inc., Berkeley, (2020), available online: https://www.csiamerica.com (accessed on February 2021).

[28] British Standards Document, BS EN 1993-4-1, Eurocode 3. Design of steel structures. Silos, (2017). doi:10.3403/30047480u.

[29] Zendaoui, Abdelhakim, A. Kadid, and D. Yahiaoui. "Comparison of Different Numerical Models of RC Elements for Predicting the Seismic Performance of Structures." International Journal of Concrete Structures and Materials 10, no. 4 (September 27, 2016): 461–478. doi:10.1007/s40069-016-0170-7.

[30] Houda, Gasmi, Bouzid Tayeb, and D. Yahiaoui. "Key Parameters Influencing Performance and Failure Modes for Interaction Soil–pile–structure System Under Lateral Loading." Asian Journal of Civil Engineering 19, no. 3 (March 20, 2018): 355–373. doi:10.1007/s42107-018-0033-4.

[31] Marabi, Bahram, and Abdul Kadir Marsono. "A Numerical and Analytical Study on Optimization and Efficiency of Structural Forms by Two-Outrigger in Tall Buildings." Malaysian Journal of Civil Engineering 28 (2016): 163-179.

[32] Hu, Yiwei, Nelson Lam, Scott Joseph Menegon, and John Wilson. "The Selection and Scaling of Ground Motion Accelerograms for Use in Stable Continental Regions." Journal of Earthquake Engineering (April 21, 2021): 1–21. doi:10.1080/13632469.2021.1913456.

[33] Bommer, J. J., and S. G. Scott. "The Feasibility of Using Real Accelerograms for Seismic Design." Implications of Recent Earthquakes on Seismic Risk (March 2000). doi:10.1142/9781848160194_0009.

[34] Shome, Nilesh. Probabilistic seismic demand analysis of nonlinear structures. Stanford University, (1999).

[35] Applied Technology Council, and United States. Federal Emergency Management Agency. Quantification of building seismic performance factors. US Department of Homeland Security, FEMA, (2009).

[36] Rota, M., A. Penna, and G. Magenes. "A Methodology for Deriving Analytical Fragility Curves for Masonry Buildings Based on Stochastic Nonlinear Analyses." Engineering Structures 32, no. 5 (May 2010): 1312–1323. doi:10.1016/j.engstruct.2010.01.009.

[37] SeismoMatch,(2021). Application capable of adjusting earthquake accelerograms to match a specific target response spectrum, available from URL: http//www.seismosoft.com.

[38] Vamvatsikos, Dimitrios, and C. Allin Cornell. "Incremental Dynamic Analysis." Earthquake Engineering & Structural Dynamics 31, no. 3 (2002): 491–514. doi:10.1002/eqe.141.

[39] Prestandard, F. E. M. A. "commentary for the seismic rehabilitation of buildings (FEMA356)." Washington, DC: Federal Emergency Management Agency 7 (2000): 2.

[40] Nesrine, Guettafi, Yahiaoui Djarir, Abbeche Khelifa, and Bouzid Tayeb. "Performance Assessment of Interaction Soil Pile Structure Using the Fragility Methodology." Civil Engineering Journal 7, no. 2 (February 1, 2021): 376–398. doi:10.28991/cej-2021-03091660.